Chapter 1.3

NOTCHED MARBLE SPECIMENS UNDER DIRECT TENSION: THE INFLUENCE OF THE SHAPE OF THE NOTCH

Zacharias G. Agioutantis[1], Stavros K. Kourkoulis[2] and George Kontos[1]
[1]Department of Mineral Resources Engineering, Technical University of Crete, 73100 Hania, Crete, Hellas, zach@ mred.tuc.gr; [2]School of Applied Sciences, Department of Mechanics, National Technical University of Athens, 5 Heroes of Polytechnion Avenue, 157 73 Zografou, Attiki, Hellas, stakkour@central.ntua.gr

Abstract: In this paper the influence of the shape of the notch on the intensity of the strain field developed in marble plates subjected to direct tension was studied both experimentally and numerically. The specimens were made from Dionysos marble, the material used for the restoration project of the Parthenon Temple of Athens. The experimental results from specimens with different notch shape were compared to each other and, also, with the respective values obtained from a numerical analysis. The material was modeled as linear elastic either isotropic or transversely isotropic. The comparison between experimental and numerical results is satisfactory concerning the specimens with the semi-circular notches. Deviations are observed for the U-shaped notch, which may be attributed to the magnitude of the process zone developed, that renders the elasticity hypothesis, adopted in the numerical analysis, invalid.

Key words: natural building stones; Dionysos marble; uniaxial tension; double edge notched specimens; finite element method.

1. INTRODUCTION

The purpose of the present study is to explore the influence of the shape of the notch on the strain field developed in double edge notched specimens made from marble when subjected to uniaxial tension. The distribution of stresses and strains in the presence of notches of various shapes concerns the engineering community for long since the stress concentration generated in the vicinity of notches is of crucial importance for the safe design of structu-

S.K. Kourkoulis (ed.), Fracture and Failure of Natural Building Stones, 35–52.

res of any kind[1]. Already from the beginning of the previous century the solutions for the stress concentration around circular and elliptic notches within an infinite plate have been introduced by Kirsch[2] and Inglis[3] respectively; however the problem in its general form is by no means closed. Particularly for cases where the assumption of infinite dimensions of the structure is not applicable, i.e. the dimensions of the plate containing the notch are of the same order of magnitude with those of the notch itself, the situation becomes extremely complicated and the analytical solutions available nowadays correspond to a limited number of special configurations. Things become worse in case the notched plate is cut from a non-isotropic material. Then the general analytical solution becomes prohibitively difficult even for the simplest degree of anisotropy, i.e. that of transverse isotropy.

Fortunately the rapid development of numerical techniques during the last two or three decades offer to the design engineers a useful tool for an at least qualitative solution of the problem, independently of the degree of complexity of the geometry analyzed. Nevertheless, as it is pointed out by Filippi and Lazzarin[4], the numerical approximations "…*lead to a typical sparse data output which is much less manageable than analytical results and, moreover, make uneasy to understand the role played by all geometrical parameters involved*". Therefore it looks like the experimental study remains the only reliable tool that can provide data necessary for the calibration and assessment of numerical models as well as for the validation of analytical attempts like the one recently introduced by Kotousov and Wang[5].

In this direction the variation of the strain-field in plates made of Dionysos marble (a typical transversely isotropic material) with either semicircular or U-shaped notches is studied here experimentally in an effort to determine the influence of the shape of the notch on the strain concentration in the vicinity of the notch tip and quantify the strain concentration factor. The results of the experimental program are then used for the calibration and assessment of a numerical model solved with the aid of the Finite Element Method and commercially available software.

2. EXPERIMENTAL PROCEDURE AND RESULTS

2.1 The material

The specimens used for the present study were cut from recently quarried marble blocks from the Dionysos Mountain in Attica, Greece. This material is used for the restoration project of the Parthenon Temple on the Acropolis of Athens because it has properties similar to those of the Pentelik marble, the authentic building material of the monument[6]. The need to study the behaviour of Dionysos marble under tension in presence of notches emanates

from the fact that a number of structural elements of the Temple (particularly architraves and capitals) are partly cracked. In addition as it was indicated by Theocaris and Koroneos[7] "*the critical stresses in case of seismic loading… are the tensile ones… at the upper part of the columns…*".

Dionysos marble is composed by 98% of calcite and it contains very small amounts of muscovite, sericite, quartz and chlorite. Its density is 2730 kg/m^3. The porosity is very low (between 0.3% in the virgin state to 0.7% after the action of natural weathering and corrosive agents). The grain size varies around 0.43×10^{-3} m and the crystals are of polygonic shape and of almost uniform size. It is of white colour with a few thin ash-green veins following the schistosity of marble and containing locally silver areas due to the existence of chlorite and muscovite[8].

From the mechanical point of view it is an orthotropic material. Series of direct tension tests[9] with cylindrical specimens cut and loaded along the three anisotropy axes indicated that the mechanical properties along the two of them are very similar to each other. Thus the material is considered as transversely isotropic described with the aid of five constants: the elastic moduli E and E′, in the plane of isotropy and normal to it, respectively, the Poisson's ratios ν and ν′ characterizing the lateral strain response in the plane of isotropy to a tensile stress acting parallel and normal to it, respectively, and G′ the shear modulus in planes normal to the plane of isotropy. The values of the elastic moduli and Poisson's ratios are shown in Table 1, together with the values of the tensile strength, σ_f.

Table 1. Mechanical constants of Dionysos marble

	E [GPa]	ν	σ_f [MPa]
Strong Direction	84.5	0.26	10.8
Intermediate Direction	79.5	0.26	9.5
Weak Direction	50.0	0.11	5.3

The axial stress-axial strain curve of Dionysos marble as obtained from the above experiments is shown in Figure 1. The material appears to be slightly bimodular, i.e. its elastic moduli in tension and compression are not exactly equal. Also, it appears to be slightly non-linear both in the tension and in the compression regime. Especially for the tension regime it was found that the stress-strain curve is accurately described by Gerstner's parabolic law[10]:

$$\sigma=E(\varepsilon-m\varepsilon^2) \quad (1)$$

where m is a numerically determined constant, equal to about 1880. The modulus of elasticity is a linearly decreasing function of strain of the form:

$$E(\varepsilon)=(1-D)Eo \quad (2)$$

In Eq.(2) D is a constant and E_o the elastic modulus at the undamaged state.

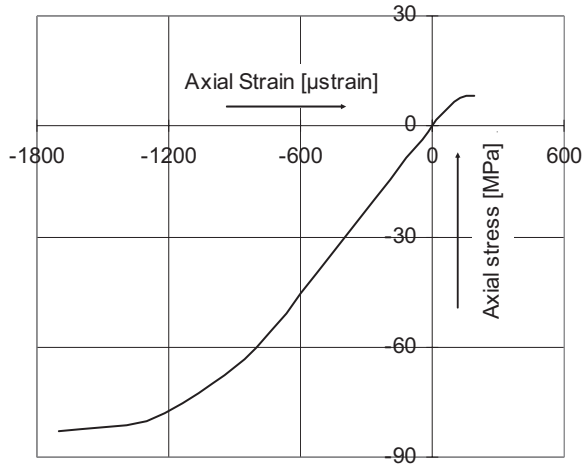

Figure 1. The axial stress - axial strain curve of Dionysos marble[9].

2.2 The specimens and the experimental procedure

Two classes of specimens were prepared. The first class included plates with two symmetric semi-circular notches of radius ρ=10 mm machined at both sides of the specimens. The geometry and dimensions are shown in Figure 2. The second class included specimens with two symmetric U-shaped notches of length a=10 mm at the vertical edges normal to the loading direction. The geometry and dimensions of these specimens are shown in Figure 3a.

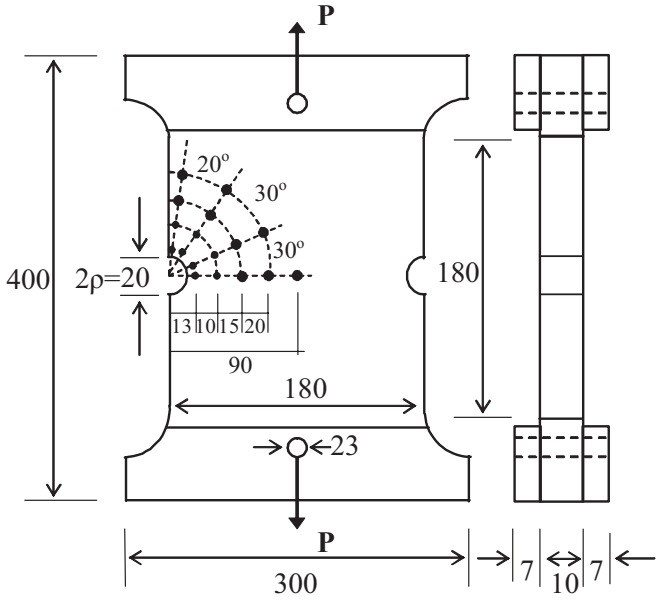

Figure 2. The geometry of the first class of specimens. The dimensions are in mm (not scaled).

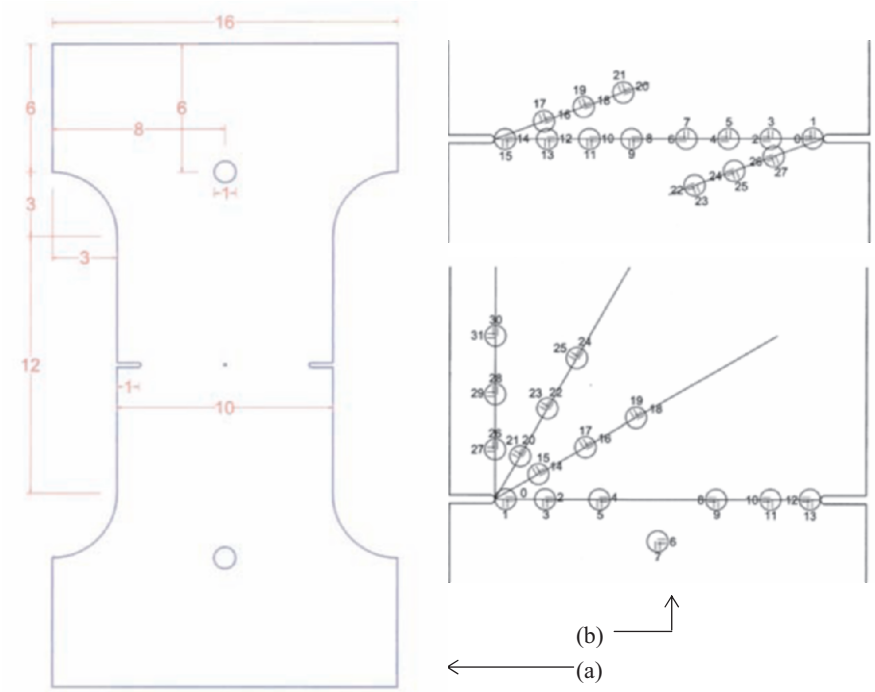

Figure 3. (a) The geometry of the second class of specimens. (b) Detailed view of the two different arrangements of the strain gauges. The dimensions are in cm.

In both cases the load was applied with the aid of two steel pins. For the first class the pins had a diameter equal to 22 mm and were mounted through holes with a diameter of 23 mm while in the second class the respective dimensions were 9 mm and 10 mm. In order to avoid fracture in the vicinity of the load-application region the "ears" of the specimens were reinforced with two pairs of plates made from plexiglas, as it is seen in Figures 2, 4 and 5b. Attention was paid to avoid direct contact of the metallic cylinders with the marble: the load was transferred from the cylinders to the marble through the adhesive material resembling thus a uniformly applied surface shear stress and avoiding stress concentration in the vicinity of the loading pin.

The plates were cut within the plane of isotropy in such a way that the load direction coincided with the strong anisotropy axis. The load was applied statically at a rate equal to 0.02 cm/min with the aid of an electric loading frame with a capacity of 250 kN. The strain components were obtained using a system of 34 strain gauges for the first class of specimens (17 orthogonal rosettes of the Kyowa KFG-X-120-D16 type) and either 28 or 32 strain gauges (14 or 16 orthogonal rosettes) for the second class of specimens. For the rosettes closest to the rim of the semi-circular notch (the ones on the circle with radius 13 mm) and the one on the tip of the U-shaped notch X=1 while for the other ones X=2. A polar system was chosen for the positioning of the strain gauges on the surface of the specimens. The exact coordinates of

the application points are shown in Figures 2 and 3b. For the specimens with U-shaped notches two arrangements of the strain gauges were used, as shown in Figure 3b. The angle between the gauge lines was 20^o for the first arrangement and 30^o for the second. The distance between the gauges was 1 cm.

A typical specimen with semi-circular notches is shown in Figures 4(a,b) just before being tested, while Figure 4c depicts the fracture surfaces of a different specimen. In Figure 5 two typical fractured specimens with U-shaped notches are shown with and without reinforced gripping zones.

(a) (b) (c)

Figure 4. (a) The front and (b) the rear view of a typical specimen with semi-circular notches just before being tested. (c) The fracture surfaces of a fractured specimen.

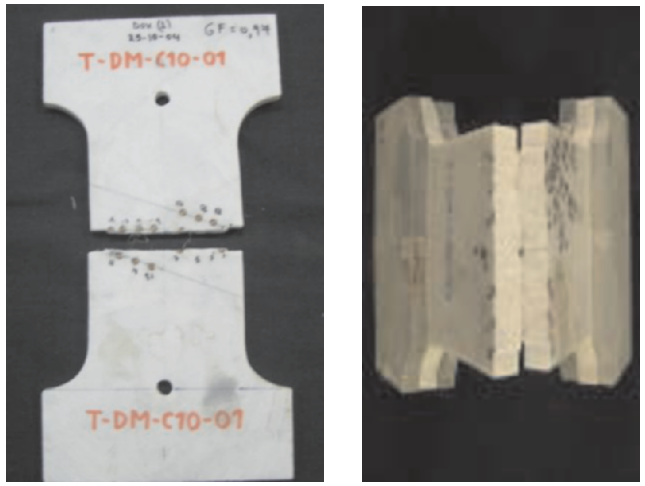

(a) (b)

Figure 5. (a) A typical fractured specimen with U-shaped notch and the first arrangement of strain gauges. (b) Fracture surfaces of a U-notched specimen with reinforced gripping zone.

2.3 Experimental results

2.3.1 Specimens with semi-circular notches

The variation of the tangential (longitudinal for $\theta=0^o$) strains developed around the notch versus the nominal stress is plotted in Figure 6a according to the results of the two rosettes positioned at $(r/\rho, \theta)=(1.3, 0^o)$ and $(r/\rho, \theta)=(9, 0^o)$, for the ultimate load $P\approx7$ kN. The specific rosettes were selected since they correspond to the point as close as possible to the notch and to the point most distanced from the notch (the center of the specimen). The strains are reduced over the maximum tangential strain developed while the nominal stress is reduced over the tensile fracture stress of the intact marble. It can be concluded from Figure 6a that for the gauge closest to the notch the evolution of the strain field is non-linear from the early loading steps, contrary to what is be expected for a quasi-brittle rock-type material. Although a slight non-linearity is reasonable according to Figure 1, it appears here that the phenomenon is not restricted for loads approaching the fracture load but it rather governs the behaviour of the Dionysos marble under tension in the presence of notches during the whole loading procedure. This non-linearity is attributed to the development of a process zone around the notch crown.

The above process zone has been quantified for Dionysos marble by Kourkoulis et al.[10,11] and its size was found to be of the order of 5-8 mm. Considering the dimensions of the rosettes used it is indeed concluded that

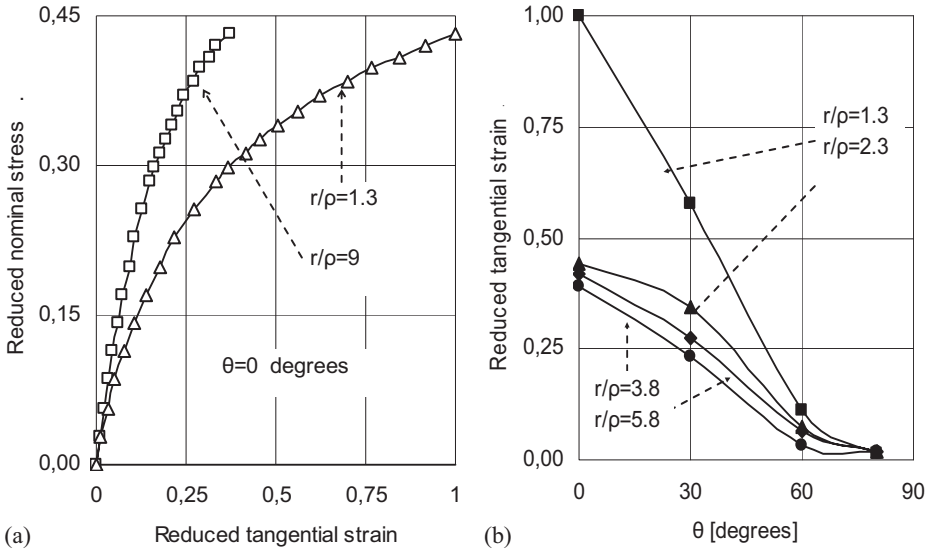

Figure 6. (a) The variation of the transverse strain vs. the remote nominal stress for the central point of the specimen and the point just ahead the notch tip. (b) The polar distribution of the transverse strain along four semi-cyclic contours with r/ρ=1.3, 2.3, 3.8 and 5.8.

the point under study lies well inside the process zone. On the contrary, at the central point of the specimen the stress-strain relation is linear for the major portion of the loading procedure and the non-linearity observed when approaching the fracture load is attributed to the nature of Dionysos marble (Figure 1). It is also seen from the same figure that the transverse strain developed in the immediate vicinity of the crown of the notch is about 2.7 times the respective strain at the central point of the specimen, providing an indication of the strain field amplification due to the presence of the notch.

In Figure 6b the polar distribution of the tangential strain component, reduced over the respective maximum value, is plotted for all four contours studied, i.e. for values of the r/ρ parameter equal to 1.3, 2.3, 3.8 and 5.8. The graphs correspond again to the ultimate value of the remotely applied load P≈7 kN. It is concluded from this figure that the influence of the notch on the strain field is restricted for r-values smaller than about two times the value of the radius ρ of the notch. In fact the differences of the transverse strains for all three contours with r/ρ=2.3, 3.8 and 5.8 are almost negligible independently from the value of angle θ and only the contour with r/ρ=1.3 diverges.

The dependence of the tangential and radial strains on the distance from the notch tip is plotted in Figures 7(a,b), respectively, where the tangential and radial strains are plotted along the linear contours θ=0°, 30°, 60° and 80°. In both figures the strains have been reduced over the maximum tangential strain developed, while the distance from the origin of the reference system (the center of the notch) is reduced over the notch radius. As it is seen from Figure 7a the transverse strain is strongly affected by the presence of the notch for the lines θ=0° and θ=30°. It is again concluded that the influence of

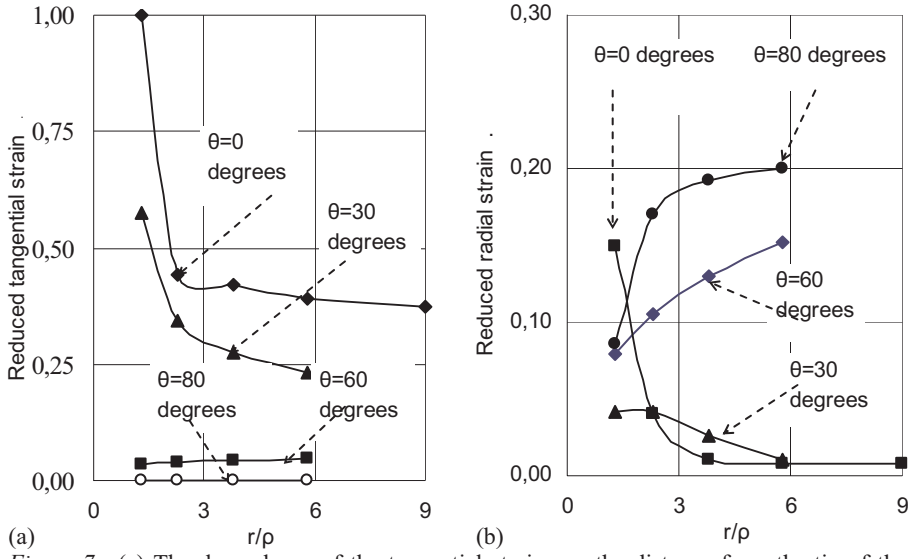

Figure 7. (a) The dependence of the tangential strains on the distance from the tip of the notch (b). The dependence of the radial strains on the distance from the tip of the notch.

the notch on the values of the transverse strain is eliminated very rapidly with increasing distance from the notch tip: indeed, for $r/\rho>2.5$ the transverse strains remain essentially constant for the whole range of θ. The variation of the radial strains is more complicated; the slope of the curves changes sign depending on the angle θ. For $\theta=0^o$ the ratio $\varepsilon_{rr}(r/\rho=1.3)/\varepsilon_{rr}(r/\rho=9)$ approaches 20 indicating a tremendous influence of the notch on the radial strain.

2.3.2 Specimens with U-shaped notches

The dependence of the tangential (longitudinal for $\theta=0^o$) and radial strains on the axial stress is shown in Figures 8(a,b), according to the data of the rosettes along the line connecting the tips of the two notches. It is again concluded that the results of the gauge closest to the tip of the notch are dramatically influenced by the notch. Indeed for both the transverse and the radial strains all three gauges at distances from the tip equal to 1.5a, 2.5a and 3.5a (a the length of the notch) give almost identical results indicating that at these points the strain field is almost uniform. In addition the stress-strain relation for these gauges is almost linear. On the contrary for the gauge with r=0.5a the stress-strain relation is strongly non-linear for both the tangential and the radial strains. It is concluded that in the case of U-shaped notches the size of the process zone for Dionysos marble varies between 5 mm and 15 mm since for the present series of tests the length of the notch is a=10 mm.

The polar distribution of the tangential and the radial strains around the tip of the notch for three semi-circular paths, with r=a, r=2.5a and r=4a are plotted for a characteristic specimen in Figures 9a and 9b, respectively. It is interesting to observe the negative values attained by the radial strains on the line

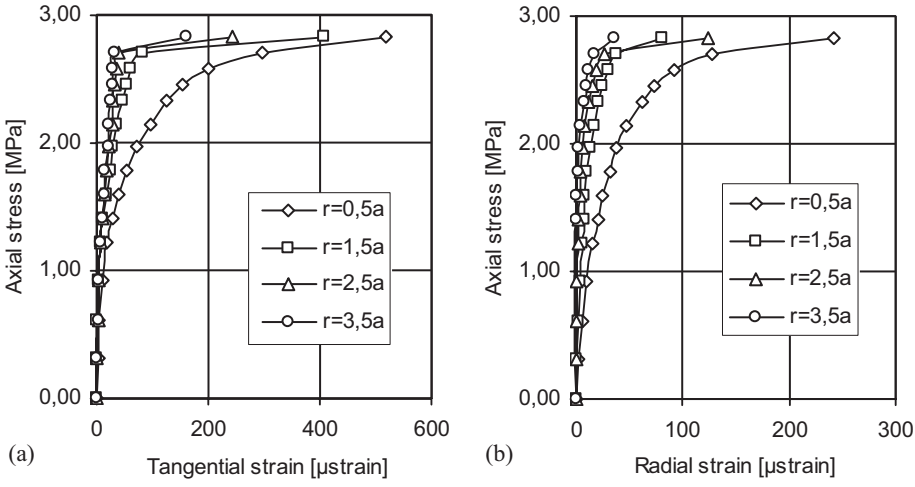

Figure 8. The variation of the transverse (longitudinal) (a) and the radial (b) strains vs. the remote axial stress for specimens with U-shaped notches at the fracture load.

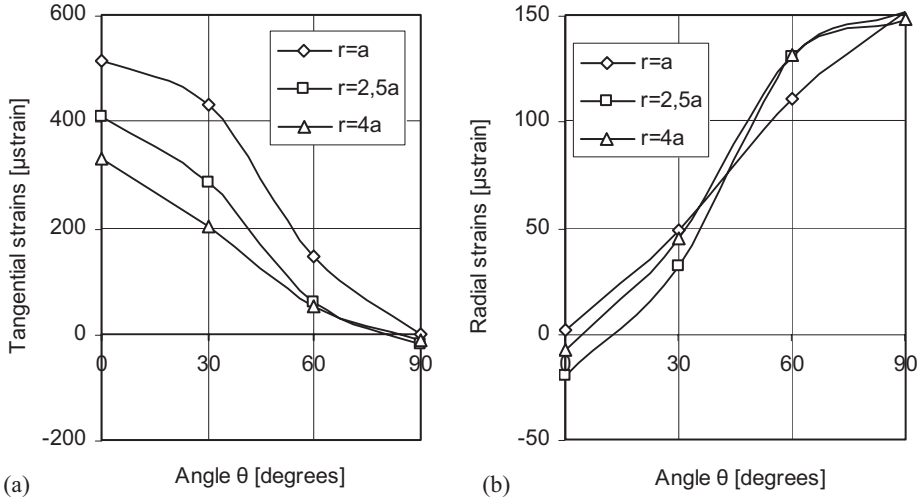

Figure 9. The polar distribution of the tangential (a) and the radial (b) strains for three semi-circular paths around the crown of the notch just before the fracture of the specimen.

with $\theta=0^o$. In addition it is stressed out that the values of the radial strains are not significantly affected by the notch, contrary to the tangential ones.

3. NUMERICAL ANALYSIS AND RESULTS

Both type of specimens described in the previous paragraph were modeled numerically in 2-D space in the MSC.Mentat front-end program, and the simulations of the tests were solved by the MSC.Marc Finite Element Analysis program[12,13]. The symmetry of the configurations was not taken into consideration. Therefore the dimensions of the final models matched exactly those of the specimens used for the experimental procedure. The model of the specimen with semi-circular notches consisted of 4502 plane stress elements and 4619 nodes while that of the specimen with U-shaped notches consisted of 7848 triangular and quadrilateral elements and 7883 nodes. In both cases the node positions were defined to coincide with the strain measuring points (the strain gauges) on the specimens in order to avoid interpolation errors.

The boundary conditions imposed include a pin-type restriction of the central node(s) of the specimens as well as distributed load on the edges. The discretization and the boundary conditions are shown in Figures 10(a,b).

The material of the specimens was modeled as linear elastic of either isotropic or orthotropic nature. Its mechanical constants matched those described in section 2.1 for Dionysos marble. The load was applied as edge load on each side of the specimen, and its total value (on both edges) corresponded to a tensile force equal to the average value of the fracture force determined experimentally for each class of specimens.

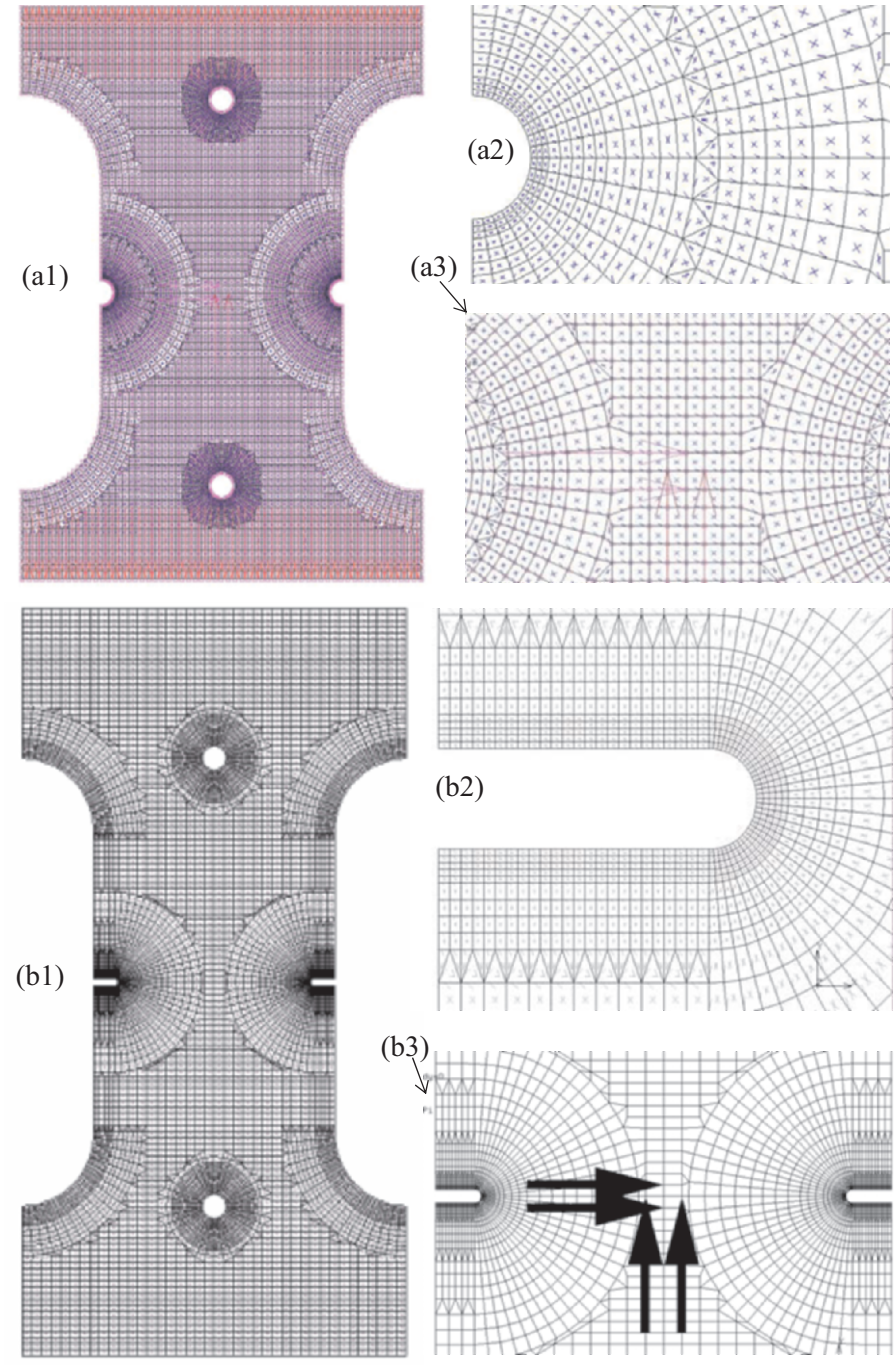

Figure 10. An overview of the numerical models of the specimens with semi-circular (a1) and U-shaped notches (b1). Details of the meshing around the crowns of the notches are also shown (a2, b2) together with the boundary conditions applied (a3, b3).

Characteristic results concerning the variation of the longitudinal (axial) strain, all over the surface of the specimens are presented in Figures 11(a,b).

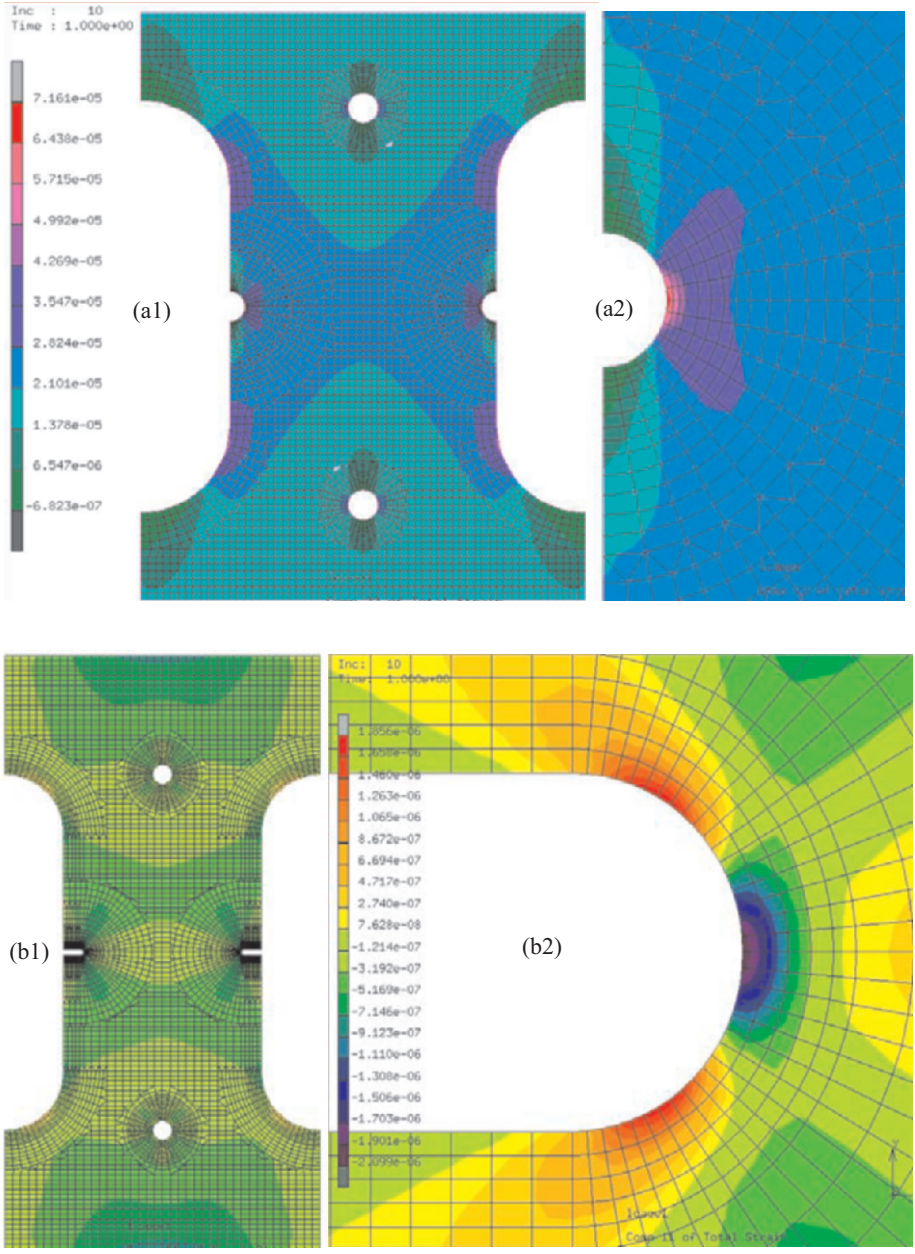

Figure 11. The distribution of the longitudinal (axial) strains ε_{yy} for the specimens with semi-circular (a1) and U-shaped notches (b1) for the isotropic model. Detailed views of the immediate vicinities of the notches are also shown in (b1) and (b2), respectively.

The variation of the normal strain components relatively to Cartesian reference systems with origins at the center of the semi-circular notch and the center of the semi-circular crown of the U-shaped notch is plotted in Figure 12. The axes of the system are parallel to the load and normal to it. For the specimens with semi-circular notches the strains are plotted along a semi-circular contour with r/ρ=1.3 encircling the notch. For the specimens with U-shaped notches the strains are plotted along a path parallel to the border line of the notch at a distance equal to r/a=1.5 from it. Both the axial (square symbols) and the transverse strains (rhombic symbols) are considered. From

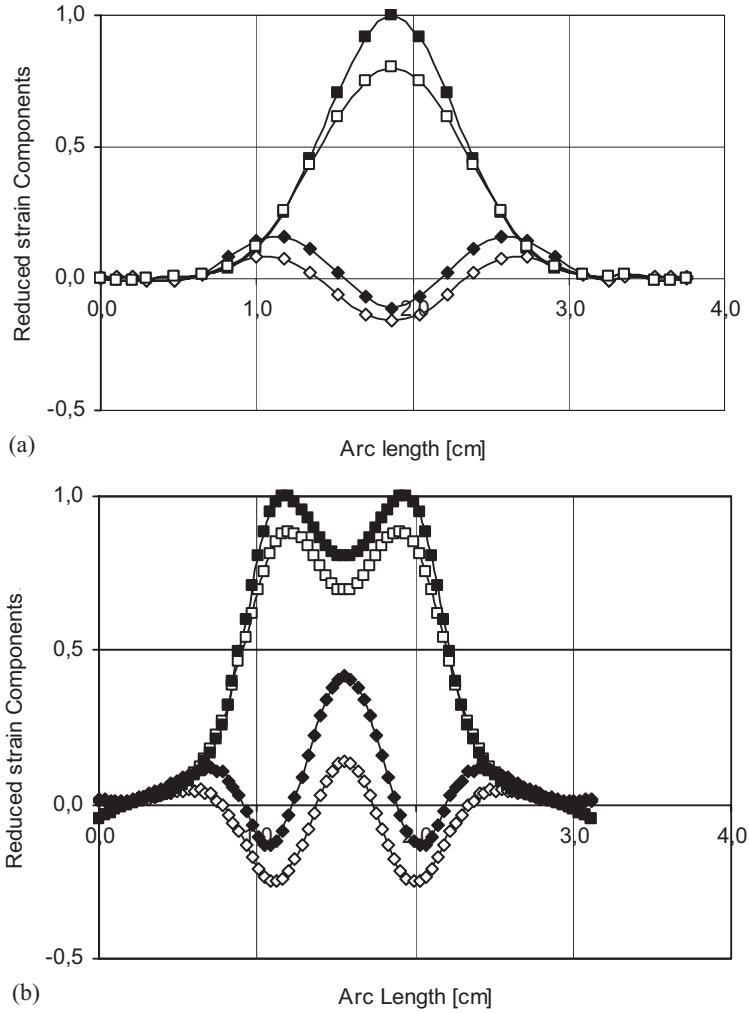

Figure 12. The variation of the normal strain components for the specimens with semi-circular (a) and U-shaped (b) notches. Filled symbols correspond to the orthotropic model while empty ones to the isotropic model. Square symbols represent the axial strains while rhombic ones represent the transverse strains.

this figure it becomes evident that the strains predicted in case the material is considered as orthotropic (filled symbols) exceed systematically those predicted from the isotropic model (empty symbols). For the specimens with semi-circular notches the difference is more pronounced for the longitudinal strains (about 20%) straight ahead from the notch tip. For the specimens with U-shaped notches the difference is more pronounced for the transverse strains (about 40%), again along the line connecting the tips of the notches.

Comparing Figures 12a and 12b it is observed that the maximum of the axial strains appears along the horizontal axis of symmetry for specimens with semi-circular notches while for the specimens with U-shaped notches two off-axis extrema appear. Although such an observation perhaps contradicts common sense it could be attributed to the finite dimensions of the specimens and the inevitable interaction between the tips of the notches. Further study is required before definite conclusions are drawn and also in order to determine the dimensions of the specimens for which the assumption of not interacting notches is valid.

4. DISCUSSION AND CONCLUSIONS

The radial distribution of the reduced axial strain along the line $\theta=0^o$ is plotted in Figure 13 as it is obtained both from the experimental measurements (empty symbols and dotted line) as well as from the numerical analysis (filled symbols and continuous lines), for the semi-circular notched specimens. The predictions of the numerical analysis are plotted both for the isotropic and the orthotropic material models (rhombic and triangular symbols,

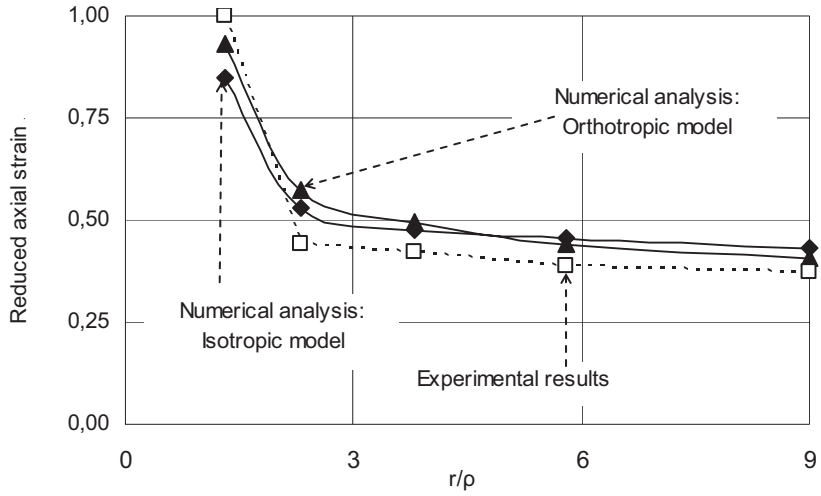

Figure 13. The radial variation of the axial strains along the line with $\theta=0^o$, according to the numerical analysis and the experimental results for the semi-circular notched specimens.

respectively). In all three cases the strains have been reduced over the respective maximum value, i.e. the value of the strain rosette at $r/\rho=1.3$, while the distance from the notch tip is reduced over the radius of the notch. It can be concluded from Figure 11 that the results of the numerical simulations are in very good agreement with those of the experimental study. The numerical results exceed slightly the experimental ones for $r/\rho>2$. From this point down the experimental results increase much more rapidly. This behaviour can be justified when considering that the linearity assumption adopted by the numerical analysis is not valid for $r/\rho<2$ since this region lies (partly or as a whole) within the process zone where intense micro-cracking is developed.

The respective results for the axial strain along the line $\theta=0^o$ for the specimens with U-shaped notches are plotted in Figure 14. Again the strains are reduced over the respective maximum value, i.e. the value of the strain rosette at $r/a=0.3$. It is seen that the results of the numerical simulations are not in such a good agreement with those of the experimental study, at least compared to the previous case. The experimental results exceed systematically those of the numerical analysis for both models and only at the center of the specimen ($r=4a$) the experimental strain is the same with that predicted by the isotropic model. These discrepancies could be expected since the strain field is more intense for the case of a U-shaped notch and therefore the non-linearity of the constitutive behaviour of marble influences a wider region around the notch. On the other hand such a result should be studied in conjunction with the conclusions drawn from Figure 8 where it was observed that the influence of the notch is restricted within an area of about 5 to 15 mm (only the results of the strain rosette closest to the tip are non-linear).

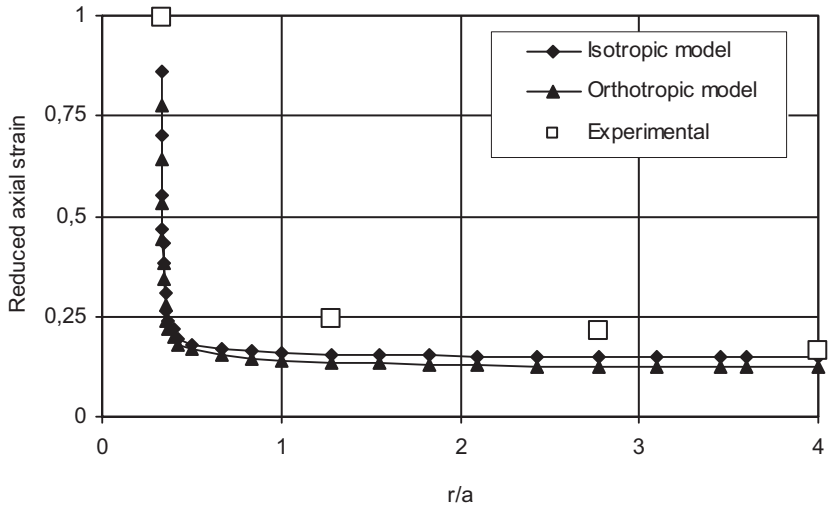

Figure 14. The radial variation of the axial strains along the line with $\theta=0^o$, according to the numerical analysis and the experimental results for the specimens with U-shaped notch.

For the specimens with U-shaped notches the distribution of the radial strain along a path parallel to the border-line of the notch at a distance equal to 11.5 mm from it, is plotted in Figure 15, according to both the numerical analysis and the experimental results. It is concluded that the isotropic model predicts strains significantly higher from those of the orthotropic one. The experimental results support the predictions of the latter. Some deviations appear only along the axis of symmetry of the notch.

The comparative study of the amplification of the strain field due to the presence of different types of notches, according to both the isotropic and the orthotropic models can be carried out with the aid of Figures 16(a,b). The comparison is carried for the strain fields developed along the horizontal axis of symmetry of the specimens, i.e. the line connecting the two tips. The origin of the x-axis is the center of the specimens and its end is the tip of the notch. In other words x/r=0 corresponds to the central point of both types of the specimens while x/r=-0.8 and x/r=-0.9 correspond to the tips of the U-shaped and the semi-circular notch, respectively.

The stress concentration factor for the semi-circular notches, defined as the axial strain developed at the center of the specimens over the respective strain at the tip of the notch, is about 2.7, while for the U-shaped notches the respective factor is equal to about 10. The predictions of the orthotropic model are, in general, higher from the respective ones of the isotropic model. The above values should not be compared with the respective ones obtained from analytical solutions since they can not take into consideration neither the fact that the specimens are of finite dimensions permitting interaction of the notches nor the exact shape of the notch.

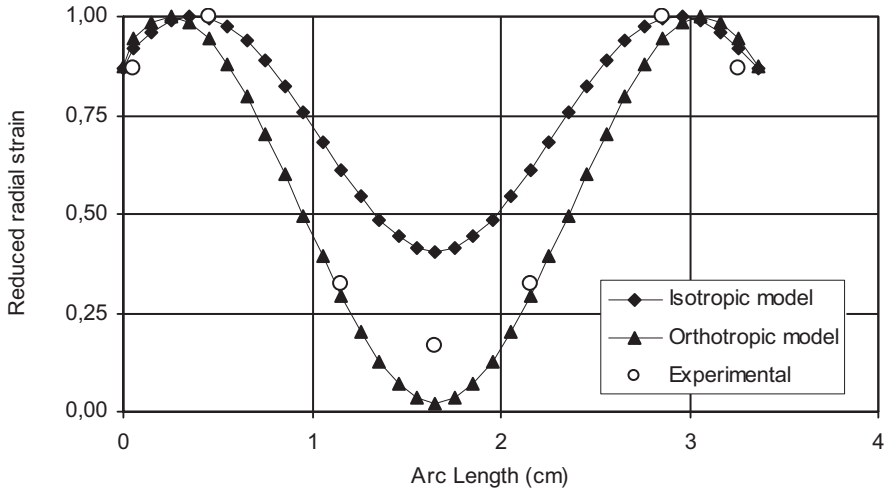

Figure 15. The variation of the radial strains along a path parallel to the border-line of the notch at a distance equal 11.5 mm from it, according to the numerical analysis and the experimental results for the specimens with U-shaped notch.

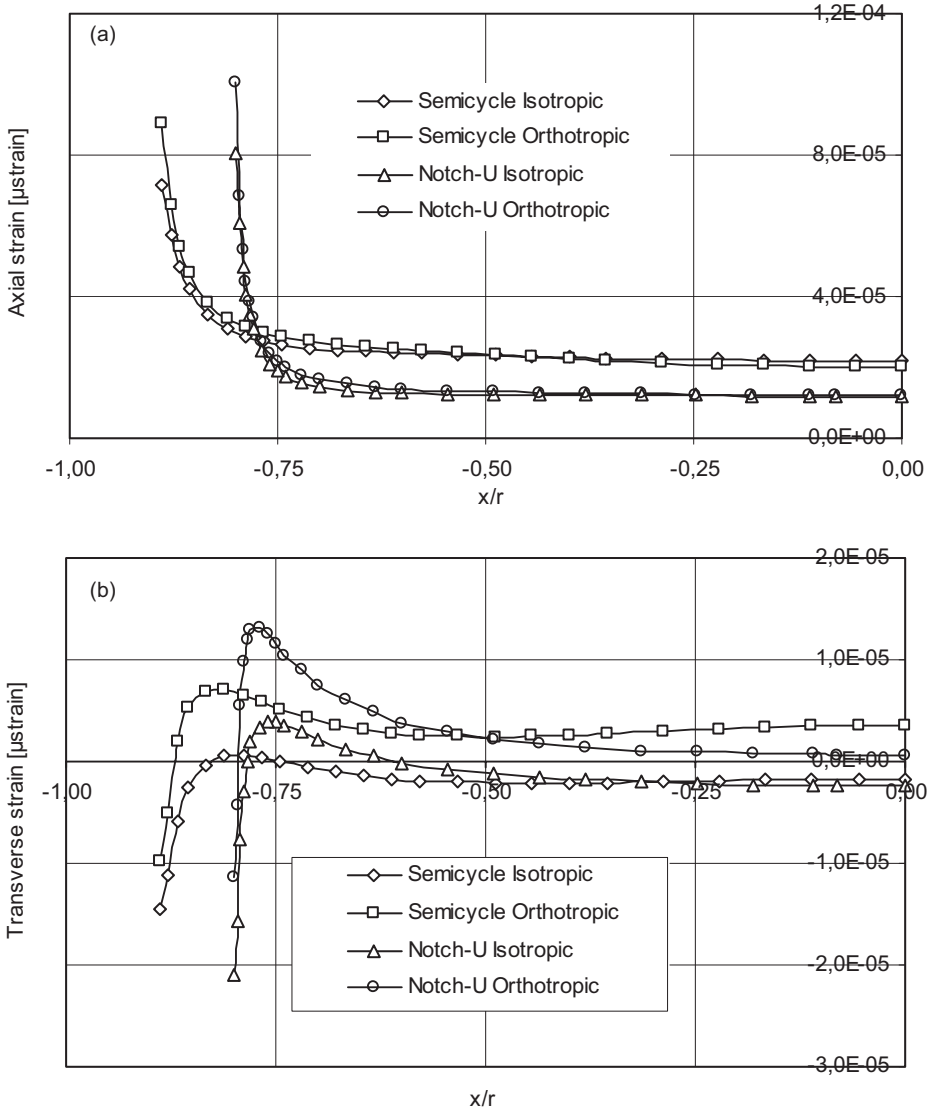

Figure 16. The variation of the axial (a) and the transverse (b) strain components along the line connecting the two notches for the different shape of the notches and for both the isotropic and the orthotropic models according to the results of the numerical analysis.

In summary, the strain field developed in marble plates with semi-circular and U-shaped notches was studied experimentally and numerically. Dogbone specimens with specially designed reinforced gripping zone were subjected to direct tension. The study revealed that:

- A process zone of intense damage (micro-cracking etc.) is developed around the notch in both cases rendering the macroscopic axial stress - axial strain relation non-linear from relatively early loading steps.

- The extent of the process zone varies between 5-8 mm for the specimens with semi-circular notches and 5-15 mm for those with U-shaped notches.
- The influence of the notch is eliminated rapidly: For $r/\rho>2$ (semi-circular notch) and $r/a>1.5$ (for the U-shaped notch) it becomes almost negligible.
- The results of the numerical analysis are in good agreement with the respective experimental ones for the case of specimens with semi-circular notches while for the ones with U-shaped notches the numerical predictions underestimate the experimental reality: Significant discrepancies are observed for points very close or inside the process zone.
- The semi-circular notch amplifies the strain field by almost 2.7 times while the U-shaped one by almost 10 times.

ACKNOWLEDGEMENTS

The authors would like to express their gratitude to Mr N. Moschakis for his help in the preparation of the specimens and the execution of the experiments. The numerical analysis is part of the Master Thesis of the third author.

REFERENCES

1. Z. H. Li and W.L. Guo, Three-dimensional elastic stress fields ahead of blunt V-notches in finite thickness plates, *Int. J. Fracture* **107**, 53-71 (2001).
2. G. Kirsh, Die Theorie der Elasticität und die Bedürfnisse der Festigkeitlehre, *Z. Ver. Dtsch. Ing.* **32**, 797-807 (1898).
3. C. E. Inglis, Stresses in a plate due to the presence of cracks and sharp corners, *Proc. Inst. Nav. Arch*. **55**(1), 219-230 (1913).
4. S. Filippi, P. Lazzarin, Distributions of the elastic principal stress due to notches in finite size plates and rounded bars uniaxially loaded, *Int. J. Fatigue* **26**, 377-391 (2004).
5. Kotousov, A., Wang, C.H., A generalized plane-strain theory for transversally isotropic plates, *Acta Mechanica* **161**, 53-64 (2003).
6. C. Zambas, Structural Repairs to the Monuments of the Acropolis-The Parthenon, *Proc. of the Institution of Civil Engineers - Civil Engineering* **92**, 166-176 (1992) (in Greek).
7. P. S. Theocaris and E. Coroneos, Experimental study of the stability of Parthenon, *Publications of the Academy of Athens* **44**, 1-80 (1979) (in Greek).
8. A. G. Tassogiannopoulos, A Contribution to the Study of the Properties of Structural Natural Stones of Greece, Ph.D. Dissertation (Nat. Techn. Univ. of Athens, 1986) (in Greek).
9. I. Vardoulakis, S. K. Kourkoulis, Mechanical Properties of Dionysos Marble, in: *Final Report of the Environment Project EV5V-CT93-0300* (Nat. Techn. Univ. of Athens, 1997).
10. S. K. Kourkoulis, G. E. Exadaktylos, and I. Vardoulakis, Notched Dionysos-Pentelicon marble in three point bending: The effect of nonlinearity, anisotropy and microstructure, *Int. J. Fracture* **98**, 369-392 (1999).
11. S. K. Kourkoulis, G. E. Exadaktylos and I. Vardoulakis, in: *Proc. 14th European Conf. on Fracture*, edited by A. Neimitz et al. (EMAS Publishing, UK 2004), pp. 243-250.
12. MARC: Analysis Research Corporation, Users' Manuals (1998).
13. Mentat 2: User's guide (1996).